Roughness exponents and grain shapes

T. J. Oliveira[1,*] and F. D. A. Aarão Reis[2,†]

[1]*Departamento de Física, Universidade Federal de Viçosa, 36570-000 Viçosa, Minas Gerais, Brazil*

[2]*Instituto de Física, Universidade Federal Fluminense, Avenida Litorânea s/n, 24210-340 Niterói, Rio de Janeiro, Brazil*

(Received 9 February 2011; published 20 April 2011)

In surfaces with grainy features, the local roughness w shows a crossover at a characteristic length r_c, with roughness exponent changing from $\alpha_1 \approx 1$ to a smaller α_2. The grain shape, the choice of w or height-height correlation function (HHCF) C, and the procedure to calculate root-mean-square averages are shown to have remarkable effects on α_1. With grains of pyramidal shape, α_1 can be as low as 0.71, which is much lower than the previous prediction 0.85 for rounded grains. The same crossover is observed in the HHCF, but with initial exponent $\chi_1 \approx 0.5$ for flat grains, while for some conical grains it may increase to $\chi_1 \approx 0.7$. The universality class of the growth process determines the exponents $\alpha_2 = \chi_2$ after the crossover, but has no effect on the initial exponents α_1 and χ_1, supporting the geometric interpretation of their values. For all grain shapes and different definitions of surface roughness or HHCF, we still observe that the crossover length r_c is an accurate estimate of the grain size. The exponents obtained in several recent experimental works on different materials are explained by those models, with some surface images qualitatively similar to our model films.

DOI: 10.1103/PhysRevE.83.041608 PACS number(s): 68.35.Ct, 05.40.−a

I. INTRODUCTION

Scaling properties of the local surface roughness w and of the height-height correlation function (HHCF) C are very useful to understand the growth dynamics of thin films and other deposits [1–3]. The usual approach is to measure exponents from plots of w or C as a function of the box size r (roughness exponent) or time t (growth exponent) and to relate their values to some universality class of growth [1]. However, a very small number of systems exhibit simple scaling features to match those theories. For instance, the presence of grains in the film surface leads to a crossover between two regimes where w increases with r with different roughness exponents α_1 and α_2, as illustrated in Fig. 1 [4–10]. For the HHCF, the same crossover occurs with exponents χ_1 and χ_2. Similar crossover is observed in other systems, such as fresh snow on the ground and pyroclastic deposits on volcanic surfaces [11,12].

In Ref. [13], the crossover with $\alpha_1 \approx 1$ was shown to be a geometric effect of the grainy surface structure and of the gliding box method (an analogous result is obtained with the box counting method). It was also shown that the crossover took place when r was close to the average grain size. If the grain surface is flat, α_1 is very close to 1, while for rounded grains it decreases to values close to 0.85 [13]. These results match those of a large number of experimental works [4–10]. However, other experimental works show film surfaces with grainy structure, the same crossover in roughness scaling or HHCF, but with much smaller exponents α_1 [14–22]. The usual interpretation for those exponents is that small-scale surface features are determined by a different growth dynamics. Indeed, even the crossover with $\alpha_1 \approx 1$ was already interpreted as an anomalous scaling, with α_1 being called the local roughness exponent (denoted $\alpha_{\rm loc}$) and α_2 called the global roughness exponent. For these reasons, in many systems it is still unclear whether a crossover similar to that in Fig. 1 should be interpreted as a purely geometric effect or as a consequence of a competitive growth dynamics.

Here we study several growth models with grainy surface features to show the possible effects of the grain shape, of the method of calculation of averages of squared quantities, of the working quantity (w or C), and of the universality class of the growth process. For all growth models, grain shapes, and methods of analysis, we observe crossovers at box sizes very close to the average grain size. We also show that a very broad range of α_1 can be found, depending on the grain shape and the working quantity, but independently of the universality class of growth, which determines only the value of α_2. Similar conclusions are obtained for the exponents χ_1 and χ_2. The comparison with experimental works with several materials and deposition methods gives additional support to the geometric interpretation of the crossover in those systems.

The rest of this work is organized as follows. In Sec. II we define average quantities and present the growth models. In Sec. III, we recall the results of some exactly solvable models with grains at the surface, which explain the crossover with $\alpha_1 \approx 1$ and $\chi_1 \approx 0.5$ (with the usual definition of the HHCF). In Sec. IV we analyze the effects of the grain shape, particularly some very sharp grains, considering models in different universality classes. In Sec. V, we show the applications of our approach to real films. In Sec. VI, we summarize our results and present our conclusions.

II. DEFINITION OF AVERAGE QUANTITIES AND MODELS

First we define the average quantities analyzed in this work. The surface roughness in square boxes of size r at time t is usually defined as

$$w(r,t) \equiv \left\langle \overline{(h-\overline{h})^2}^{1/2} \right\rangle. \quad (1)$$

The overbars in Eq. (1) denote averages of the height h inside a given box position (spatial average) and the angular brackets

*tiago@ufv.br
†reis@if.uff.br

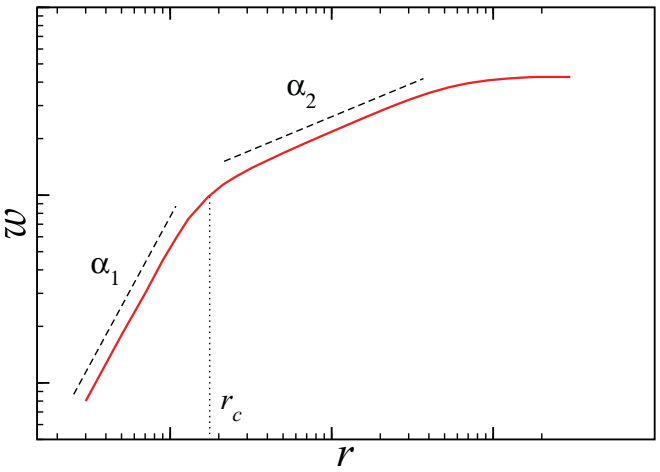

FIG. 1. (Color online) Typical behavior of the local roughness as a function of box size in grainy surfaces.

represent the configurational average as the box scans the whole surface of a deposit. This is called the gliding box method, in which the scanning box moves one pixel each time it performs a new spatial average. In box counting methods, the surface is divided into nonintersecting boxes for the configurational average.

Alternatively, some authors define the roughness as

$$w' \equiv \overline{\left\langle (h-\overline{h})^2 \right\rangle}^{1/2}, \tag{2}$$

i.e., they calculate the configurational average of the square height fluctuation and take the square root of that average.

When several images of a deposit are available, or several configurations are grown with the same model, these different samples also contribute to the above configurational averages.

For window sizes below the grain size, the roughness scales as

$$w(r,t) \sim r^{\alpha_1}, \tag{3}$$

which defines the initial roughness exponent α_1 (Fig. 1). The height-height correlation function at distance r and time t is usually defined as

$$C(r,t) \equiv \langle [h(r_0+r,t) - h(r_0,t)]^2 \rangle^{1/2}, \tag{4}$$

with configurational averages taken over all different initial positions r_0. Alternatively, it can be defined as

$$C'(r,t) \equiv \langle |h(r_0+r,t) - h(r_0,t)| \rangle, \tag{5}$$

which corresponds to an interchange of the configurational average and the calculation of the square root in Eq. (4). In this sense, the calculation of $C(r,t)$ parallels that of w', while the calculation of $C'(r,t)$ parallels that of w.

For window sizes below the grain size, the HHCF scales as

$$C(r,t) \sim r^{\chi_1}, \tag{6}$$

which defines the initial roughness exponent χ_1 for that function. For window sizes much larger than the grain size (i.e., $r \gg r_c$—see Fig. 1), a surface obeying normal scaling has $w \sim r^{\alpha_2}$ and $C \sim r^{\chi_2}$, with $\alpha_2 = \chi_2$. The quantities w' and C' obey the same scaling. Those exponents are representative of the large-length-scale kinetics governing the growth process. Typical examples of growth kinetics are those of Edwards and Wilkinson (EW) [23] and of Kardar, Parisi, and Zhang (KPZ) [24], and the diffusion-dominated ones, linear [Mullins and Herring (MH) [25]] or nonlinear [Villain, Lai, and Das Sarma (VLDS) [26,27]].

Now we present the models for growth of thin films with grains at the surface. Intrinsic corrections to scaling for large r and large t should be avoided in those models, so that any crossover is solely due to the grainy structure. This constraint excludes the grain deposition models introduced in Ref. [13] and related ballisticlike models [28,29] because they have remarkable scaling corrections. On the other hand, some models with smooth surfaces and particle enlargement presented in Refs. [7,13] satisfy that condition. They are described below.

The first model has KPZ kinetics. The first step is to grow a deposit with cubic particles of unit size following the rules of the restricted solid-on-solid (RSOS) model: the aggregation of the incident particle is accepted only if the height differences of nearest neighbors are always 0 or 1 (otherwise the aggregation attempt is rejected) [30]. We recall that $\alpha_2 = \chi_2 \approx 0.39$ for the KPZ class in two-dimensional substrates [31].

The second model has VLDS kinetics. The initial deposit is grown with the rules of the conserved restricted solid-on-solid (CRSOS) model, where the incident particle executes a random walk between neighboring columns until finding a column where it can aggregate, respecting the conditions on height differences [32,33]. We recall that $\alpha_2 = \chi_2 \approx 0.67$ for the VLDS class in two-dimensional substrates [33,34].

After growing the initial deposit, with the KPZ or VLDS model, the size of each particle is enlarged by a factor l, i.e., each particle is transformed into a cubic grain of side l. Most of our simulations are performed with $l = 32$. The final step is replacing the top cube grains (surface grains) by rounded or sharp structures. Three shapes are used: semiellipsoids of horizontal radius $l\sqrt{2}/2$ and vertical radius h, cones with that radius and height h, and pyramids of square basis of side l and height h. They are illustrated in Fig. 2. Several values of h are considered for each shape, typically between l and $3l$.

In the scaling of w or C, the role of the height h depends on its size relative to the height of the surface steps, which is l. The horizontal scaling factor is also l for the cubic grains, but this is not important for the scaling exponents. For instance, if the grains were constructed with the shape of parallelepipeds of height l and horizontal side $l_\parallel$, the scaling exponents would not change. Thus, the aspect ratio of the grains considered here is not a limitation of the model.

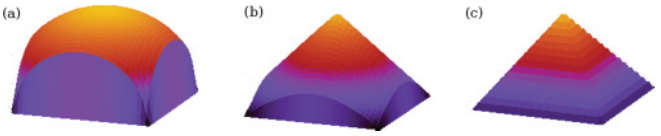

FIG. 2. (Color online) Shapes of surface grains after enlargement of the original deposits: (a) semielliptical, (b) conical, and (c) pyramidal. Semiellipsoids and cones are cut at the sides so that their bases are squares of side l that fit the shape of the cubic grain at their bottom. This is the reason for the radius $l\sqrt{2}/2$ of their bases.

The simulations of the KPZ and VLDS models were performed on square substrates (three-dimensional deposits) of lateral size $L = 128$ at times of order 10^4. For the RSOS model, it corresponds to approximately 5×10^3 layers of unit size particles; for the CRSOS model, it corresponds to 10^4 layers. After replacement of the original particles by grains of size $l = 32$, the deposits have lateral size 4096. Simulations in smaller sizes ($L = 64$ and 32 for the original models) and with different grain size ($l = 16$) give similar results for all exponents, indicating that finite-size and finite-time effects are negligible.

III. THEORETICAL PREDICTIONS FOR α_1 and χ_1

As the scanning box glides along the surface, it frequently encloses high surface steps created between neighboring grains. These are the box positions where the largest height fluctuations are encountered; thus they give the main contribution to the roughness [Eq. (1) or (2)]. If the box has size r (i.e., r pixels in each direction), then the number of box positions that involve each high step is proportional to r. Thus, the configurational average of Eq. (1) gives roughness w proportional to r. This gives $\alpha_1 = 1$, as explained in Ref. [13] and confirmed by simulations of several models.

When Eq. (2) is used, w'^2 is a configurational average. The main contribution to that average also comes from box positions enclosing high surface steps; thus, that average is proportional to r. This gives w' proportional to $r^{1/2}$, i.e., $\alpha_1 = 1/2$.

These results are confirmed by our simulations of the RSOS model with cubic grains, as shown in Fig. 3(a). It clearly shows the remarkable difference in the scaling of w and w' for box sizes smaller than the grain size, while the same exponent α_2 after the crossover represents the universality class of the process.

A similar situation is observed with the HHCF. Again the main contribution for the configurational average comes from box positions which involve high surface steps; thus this average is proportional to r. With the most used definition of that function [Eq. (4)], we have $C(r,t)$ proportional to $r^{1/2}$, and thus the crossover takes place with $\chi_1 = 1/2$. Instead, if the scaling of $C'(r,t)$ is analyzed, we expect $\chi_1 = 1$.

Simulations of the RSOS model with cubic grains show the predicted crossover, as illustrated in Fig. 3(b). The exponent χ_1 is very close to 1/2 for $C(r,t)$ and slightly below 1 for $C'(r,t)$. Again, the universal exponent χ_2 is obtained after the crossover; as expected, $\alpha_2 \approx \chi_2$.

With the usual definitions of surface roughness [w, Eq. (1)] and HHCF [C, Eq. (4)], the roughness exponents measured before the crossover (α_1,χ_1) are different. This contrasts with the expected universality after the crossover ($\alpha_2 \approx \chi_2$). Our analysis shows that those discrepancies are effects of the grainy morphology and the calculation method, in particular the order of calculation of the square root and configurational average in Eqs. (1) and (4).

IV. EFFECTS OF GRAIN SHAPE

Rounding of the surface grains may lead to α_1 between 0.85 and 1, as shown in Ref. [13]. However, the replacement

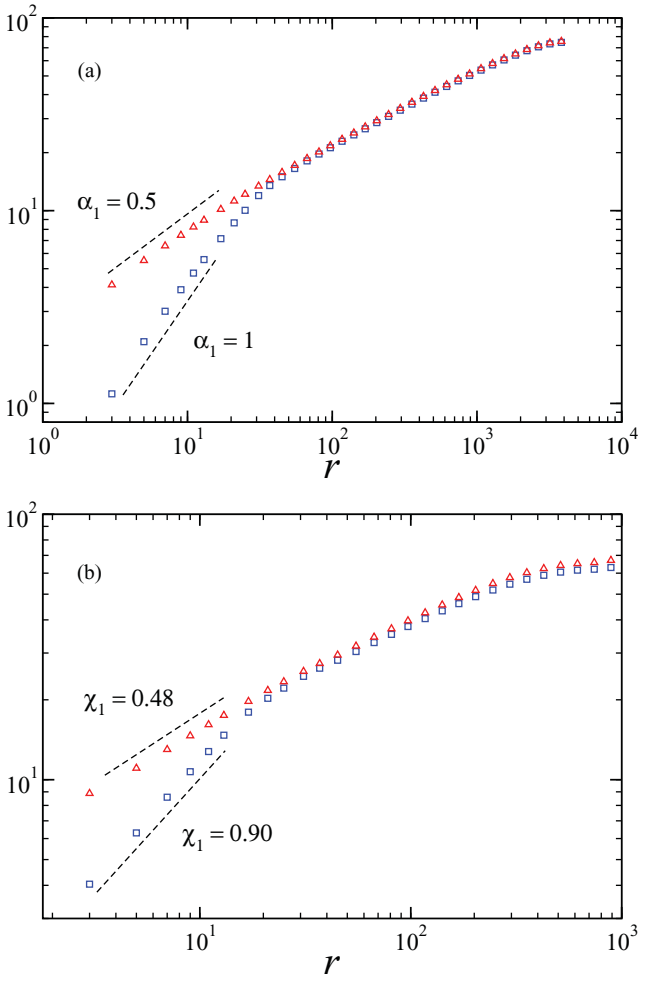

FIG. 3. (Color online) Scaling with the window size r of data for the KPZ model with cubic grains: (a) w (blue squares) and w' (red triangles); and (b) C' (blue squares) and C (red triangles).

of the cubic grains by the rounded or sharp structures in Fig. 2, with $h \geqslant l$, leads to much more drastic changes in the initial exponents of $w(r,t)$ and $C(r,t)$.

This result is illustrated in Figs. 4(a) and 4(b) for films grown with the KPZ model and pyramidal grains of height $h = 64$: α_1 decreases to 0.71 and χ_1 increases to 0.61 (while $\alpha_2 \approx 0.39$). Figure 4(b) also shows the formation of a plateau in the HHCF before the second scaling regime, which is characteristic of all sharp grains with large heights.

In Table I, we show the values of α_1 and χ_1 obtained for semielliptical, conical, and pyramidal grains with several heights. A remarkable result is that films grown with the VLDS model have the same exponents α_1,χ_1 up to the second decimal place, despite the significant change in the asymptotic roughness exponent ($\alpha_2 \approx 0.67$). In Figs. 5(a) and 5(b), we show results for conic grains with height $h = 32$, which give $\alpha_1 = 0.809$ and $\chi_1 = 0.539$. Those values are close to the KPZ values shown in Table I for the same grains. The main differences from the models with KPZ scaling are that the change in the slope of the roughness plot is smaller and there is a slope increase in the HHCF plot when passing from the first to the second scaling regime.

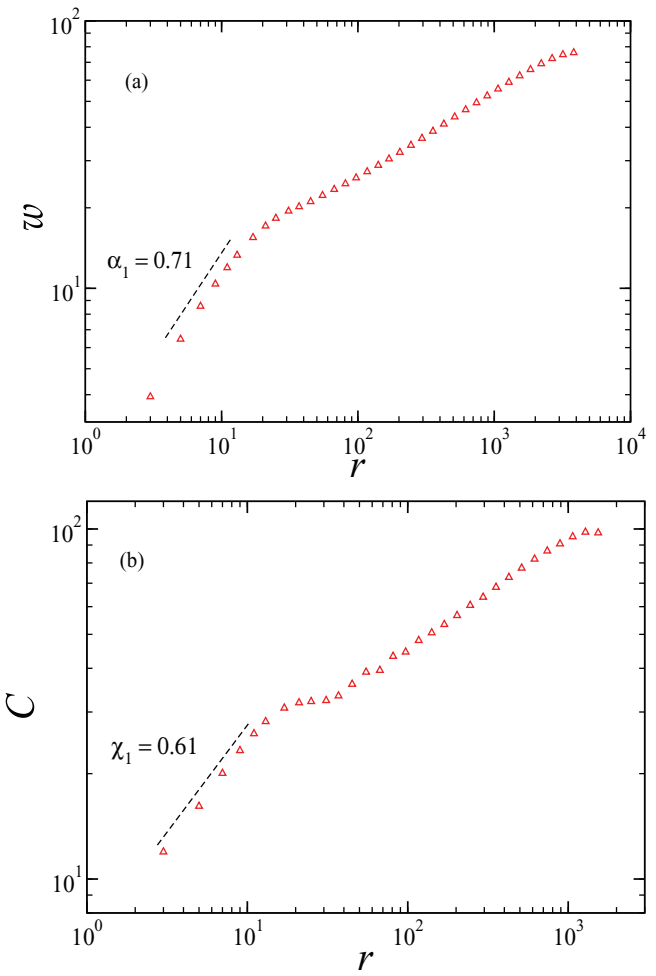

FIG. 4. (Color online) (a) Roughness (w) and (b) HHCF (C) as a function of the window size r, for the KPZ model with pyramidal grains of height $h = 64$.

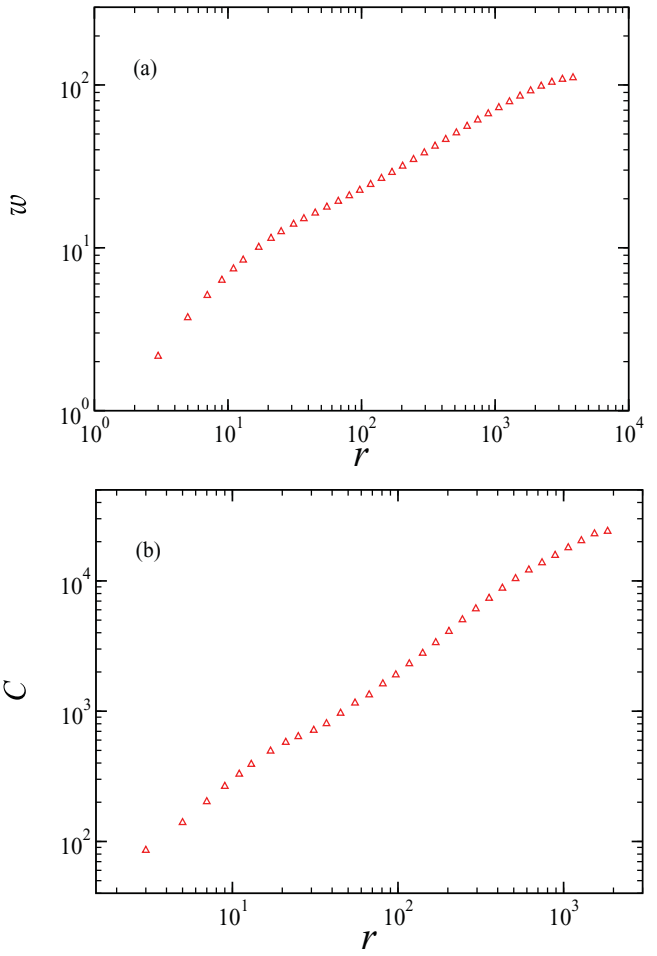

FIG. 5. (Color online) (a) Roughness (w) and (b) HHCF (C) as a function of the window size r, for the VLDS model with conical grains of height $h = 32$.

Table I shows that α_1 is much smaller than the limit 0.85 obtained in previous work [13] for many grain shapes, particularly for sharp conic and pyramidal grains. With the structures studied here, the lower limit is close to 0.71, obtained with pyramidal grains. For $h \leqslant 3l$, the general trend is that the increase of h leads to decrease of α_1. For larger h (not shown in Table I), a very slow increase of α_1 toward 1 is observed.

The relative changes in χ_1 are much larger, attaining almost 40% for conic grains with $h = 3l$ (see Table I). Indeed, this is the grain shape that provides higher deviations from the flat grain value $\chi_1 = 0.5$. A monotonic increase of χ_1 is observed when taller grains are studied.

The above results show that sharp grain shapes bring the exponents α_1 and χ_1 closer together, in contrast with the very different values for flat grains (1 and 0.5, respectively; Sec. III). In some cases, they are surprisingly close; for instance, they differ by only 10% for conic grains with $h = 3l$.

In Table II, we show exponents α_1 and χ_1 obtained from the scaling of $w'(r,t)$ and $C'(r,t)$. They should be compared with the respective flat grain values 0.5 and 1.

TABLE I. Exponents obtained from w (α_1) and C (χ_1) in KPZ films with semielliptical (SE), conical (C), and pyramidal (P) grains.

h	32	64	96
α_1^{SE}	0.826	0.773	0.763
χ_1^{SE}	0.504	0.551	0.589
α_1^{C}	0.806	0.768	0.768
χ_1^{C}	0.539	0.633	0.694
α_1^{P}	0.755	0.710	0.708
χ_1^{P}	0.535	0.606	0.645

TABLE II. Exponents obtained from w' (α_1) and C' (χ_1) in KPZ films with semielliptical (SE), conical (C), and pyramidal (P) grains.

h	32	64	96
α_1^{SE}	0.523	0.576	0.621
χ_1^{SE}	0.754	0.711	0.705
α_1^{C}	0.554	0.650	0.719
χ_1^{C}	0.712	0.693	0.710
α_1^{P}	0.556	0.638	0.687
χ_1^{P}	0.664	0.633	0.640

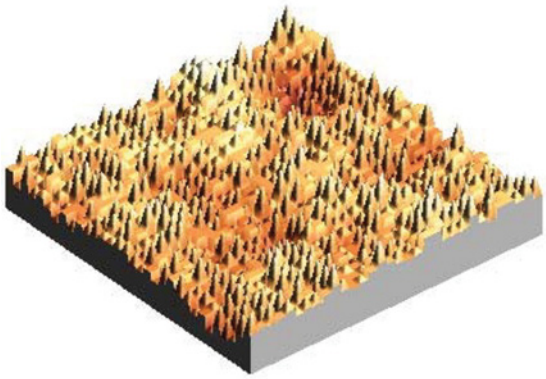

FIG. 6. (Color online) Film surface with 1/4 of the grains flat and 3/4 pyramidal with heights $h = 32$, 64, and 96 equally distributed.

Comparison of results in Tables I and II shows that sharp grain shapes also bring closer the values of α_1 measured from w and w' scaling, which are very different for flat grains (1 and 0.5, respectively; Sec. III). It is particularly interesting to observe that α_1 differs by only 3% when calculated from w or w' in films with pyramidal shapes with $h = 3l$. These values may be incorrectly interpreted as true roughness exponents because the same α_2 is expected for w and w'. This type of erroneous interpretation can be avoided if one accounts for the effects of a wide range of grain shapes and sizes and investigates other quantities, such as the HHCF.

The crossover size r_c is defined at the intersection of the linear fits of the initial regime and the second scaling regime of roughness or HHCF, as illustrated in Fig. 1. Despite the wide range of values of α_1 and χ_1 shown in Tables I and II, a remarkable result is that r_c is always very close to the grain size l, for the KPZ and VLDS models. Using $l = 32$, our estimates range between $r_c = 30$ and $r_c = 34$, which corresponds to a maximum difference of 7%. Consequently, r_c can always be used as a reliable estimate of the grain size.

In the above models, we considered surfaces with uniform grain height. However, we also analyzed the effect of distributions of grain heights, since this is the situation in real surfaces. In all cases, we observe that the exponents α_1 and χ_1 are near the averages of those obtained with a single value of grain height.

An example of a film surface with such random grain distribution is shown in Fig. 6: 1/4 of the grains are flat and 3/4 have pyramidal shape, with equally distributed heights $h = 32$, 64, and 96. For that surface, we obtain $\alpha_1 = 0.742$ and $\chi_1 = 0.554$, which is close to the average of the results in Table I for those shapes.

V. COMPARISON WITH EXPERIMENTAL RESULTS

In the experimental works discussed below, the exponent α_1 defined here is frequently named the local roughness exponent $\alpha_{\rm loc}$, as a reference to the small-length-scale behavior and/or to a possible anomalous scaling. Several experimental works have already shown the crossover of Fig. 1 with $\alpha \approx 1$, which is explained by the growth models with flat or slightly rounded grains [13]. Among those works, we highlight the study of rf-sputtered $LiCoO_x$ films by Kleinke *et al.* [5], which gives $0.91 \leqslant \alpha_1 \leqslant 0.95$; the spray pyrolysis growth of ZnO films by Ebothé *et al.* [6], which gives $0.94 \leqslant \alpha_1 \leqslant 0.97$ for high flow rates; the electrodeposition of cooper by Mendez *et al.* [8] and of gold by Vázquez *et al.* [7], which give $\alpha_1 = 0.87 \pm 0.06$ and $\alpha_1 = 0.90 \pm 0.06$, respectively; the electrochemical roughening of silver electrodes by Otsuka and Iwasaki [9], which gives α_1 between 0.95 and 0.98; and the pulsed laser deposition of La-modied $PbTiO_3$ films of Vasco *et al.* [10], which have $\alpha_1 = 1$.

However, many works show the same crossover with exponents α_1 between 0.7 and 0.85, and surface images confirm the presence of grains of approximately conic or pyramidal shape, much higher than the steps between neighboring grains. These features are observed in films of various materials and substrates, deposited with different techniques. This justifies our approach with geometrical models, independently of the particular growth dynamics.

Among the applications to inorganic materials, we find some vapor-deposited gold films by Vazquez *et al.*, which have $\alpha_1 \approx 0.83$—see Fig. 1(c) and Fig. 3 of Ref. [14]. One of the niquel oxide film samples deposited by sputtering in Ref. [15] has $\alpha_1 = 0.70$, and the atomic force miscroscopy (AFM) image shows the qualitative features of our models with sharp grainy structure. Nearly the same exponent ($\alpha_1 = 0.71$) is obtained with Ni films electrodeposited on indium tin oxide substrates in Refs. [16,17]. Several Ni-Zn alloy films of Ref. [18] show the crossover in roughness scaling, with most estimates of α_1 in the range [0.80,0.83]. This is consistent with our models of semielliptical grains of lower h, and the images actually show a smooth grain morphology.

The same features are also observed in organic materials. Films formed with bilayers of poly(allylamine hydrochloride) and a side-chain-substituted azobenzene copolymer (Ma-co-DR13), after deposition of 10 or 20 bilayers, show grains with a broad size distribution, and the initial roughness exponents 0.81 and 0.79 [19]. AFM images of chemically deposited polyaniline thin films on glass substrates [20] have similar features, but, as far as we know, roughness scaling was not studied with those images. The surfaces of Langmuir-Blodgett films of polyaniline and a neutral biphosphinic ruthenium complex (Rupy) of Ref. [21] also show those grainy features with some high peaks, and initial roughness exponents are in the range $0.66 \leqslant \alpha_1 \leqslant 0.81$ for thicknesses between 1 and 21 layers. However, most estimates of α_1 are between 0.72 and 0.76 [21], in good agreement with our results for pyramidal grains.

It is interesting to observe that some surface images shown in Refs. [16,17,19–21] have features similar to the model illustration in Fig. 6 (in most cases without the flat grains). This comparison reinforces our interpretation of the exponents measured in those works.

Similar results are obtained in etching of silicon surfaces in Ref. [22]: α_1 is found between 0.70 and 0.87 when the (111) surface is etched by an NaOH solution in contact with a non-saturated aqueous environment.

It is also important to recall that there are systems with crossover in the roughness scaling which do not show the sharp grainy features of our models, and consequently deserve separate investigation. For instance, the image of another sample from Ref. [15] does not show those features, but the

roughness shows a slow crossover with $\alpha_1 = 0.52$. Pyroclastic deposits of Mt. Etna show roughness scaling crossover with α_1 between 0.47 and 0.67, but the images do not support modeling by grainy structures [12]. There are also systems with sharp grainy structures and small α_1, such as some Ni films of Ref. [17] ($0.55 \leqslant \alpha_1 \leqslant 0.61$), which also would deserve a separate investigation (those films have $0.12 \leqslant \alpha_2 \leqslant 0.22$, which also cannot be easily explained with the well-known kinetic growth theories [1]).

The crossover in HHCF scaling obtained in some systems can also be related to our models. For instance, Manes *et al.* [11] used HHCF as a measure of fresh snow roughness and obtained χ_1 between 0.58 and 0.62 in a set of five experiments. These values are consistent with our model with very high semiellipsoidal grains ($h = 3l$) or with conic or pyramidal grains with $h = 2l$ or less.

Again, there are also systems where a crossover of HHCF scaling is observed but whose images do not show the features of our models. An example is shown in Ref. [35], where $\chi_1 = 0.84$ was obtained for paraffin films deposited on stainless steel covered with amorphous carbon.

Results of the recent work on pentacene island growth on stepped oxide surfaces [36] can also be related to our models. First, for long lengths, the HHCF has exponent $2\chi = 1$, which is expected for height fluctuations dominated by the surface steps; indeed, arguments analogous to those for flat grains (Sec. III) give $\chi = 1/2$. However, for small lengths, height fluctuations in the surface terraces (due to pentacene islands) lead to the increase of the HHCF exponent to the range [0.69,0.8]. Recent works showing evidence of anomalous scaling in organic and inorganic film surfaces also give estimates of HHCF exponents above $1/2$ at short length scales [37,38]. Although both short- and long-range dynamics may be much more complex than in our models, a simple geometric interpretation of the short-range exponents may also be considered due to the presence of grainy structures in the surface images.

VI. CONCLUSION

We extended the work on growth models with grainy surfaces to analyze the effects of the grain shape, of the method of calculation of averages of squared quantities, of the working quantity (roughness or HHCF), and of the universality class of the growth process. For all models, grain shapes, and methods of analysis, we observe crossovers at box sizes very close to the average grain size. We also show that a very broad range of the initial exponent α_1 is found for the roughness scaling, decreasing from 1 for flat grains to 0.71 for some sharp pyramidal grains. The initial exponent χ_1 of HHCF scaling increases from approximately 0.5 for flat grains to values larger than 0.7 for sharp conic grains. Simulations of KPZ and VLDS models show that the universality class has no significant effect on the estimates of α_1 and χ_1. The range of α_1 presented here explains results of some recent experimental works with different materials and deposition methods. This gives additional support to the geometric interpretation of the crossover in roughness scaling for a variety of systems.

ACKNOWLEDGMENTS

F.D.A.A.R. acknowledges support from CNPq and Faperj (Brazilian agencies).

[1] A. L. Barabási and H. E. Stanley, *Fractal Concepts in Surface Growth* (Cambridge University Press, Cambridge, England, 1995).
[2] J. Krug, Adv. Phys. **46**, 139 (1997).
[3] J. Krim and G. Palasantzas, Int. J. Mod. Phys. B **9**, 599 (1995).
[4] A. E. Lita and J. E. Sanchez, Jr., Phys. Rev. B **61**, 7692 (2000).
[5] M. U. Kleinke, J. Davalos, C. Polo da Fonseca, and A. Gorenstein, Appl. Phys. Lett. **74**, 1683 (1999).
[6] J. Ebothé, A. El Hichou, P. Vautrot, and M. Addou, J. Appl. Phys. **93**, 632 (2003).
[7] L. Vázquez, R. C. Salvarezza, P. Herrasti, P. Ocón, J. M. Vara, and A. J. Arvia, Phys. Rev. B **52**, 2032 (1995).
[8] S. Mendez, G. Andreasen, P. Schilardi, M. Figueroa, L. Vázquez, R. C. Salvarezza, and A. J. Arvia, Langmuir **14**, 2515 (1998).
[9] I. Otsuka and T. Iwasaki, J. Vac. Sci. Technol. B **14**, 1153 (1996).
[10] E. Vasco, C. Polop, and C. Ocal, Eur. Phys. J. B **35**, 49 (2003).
[11] C. Manes, M. Guala, H. Lowe, S. Bartlett, L. Egli, and M. Lehning, Water Resour. Res. **44**, W11407 (2008).
[12] F. Mazzarini, M. Favalli, I. Isola, M. Neri, and M. T. Pareschi, Ann. Geophys. **51**, 813 (2008).
[13] T. J. Oliveira and F. D. A. Aarão Reis, J. Appl. Phys. **101**, 063507 (2007).
[14] L. Vázquez, R. C. Salvarezza, P. Herrasti, P. Ocón, J. M. Vara, and A. J. Arvia, Surf. Sci. **345**, 17 (1996).
[15] T. G. S. Cruz, M. U. Kleinke, and A. Gorenstein, Appl. Phys. Lett. **81**, 4922 (2002).
[16] L. Nzoghe-Mendome, A. Aloufy, J. Ebothé, M. El Messiry, and D. Hui, J. Cryst. Growth **311**, 1206 (2009).
[17] L. Nzoghe-Mendome, A. Aloufy, J. Ebothé, D. Hui, and M. El Messiry, Mater. Chem. Phys. **115**, 551 (2009).
[18] M. Hiane and J. Ebothé, Eur. Phys. J. B **22**, 485 (2001).
[19] N. C. de Souza, V. Zucolotto, J. R. Silva, F. R. Santos, D. S. dos Santos Jr., D. T. Balogh, O. N. Oliveira Jr., and J. A. Giacometti, J. Colloid Interface Sci. **285**, 544 (2005).
[20] S. A. Travain, N. C. de Souza, D. T. Balogh, and J. A. Giacometti, J. Colloid Interface Sci. **316**, 292 (2007).
[21] N. C. de Souza, M. Ferreira, K. Wohnrath, J. R. Silva, O. N. Oliveira Jr., and J. A. Giacometti, Nanotechnology **18**, 075713 (2007).
[22] M. E. R. Dotto and M. U. Kleinke, Phys. Rev. B **65**, 245323 (2002).
[23] S. F. Edwards and D. R. Wilkinson, Proc. R. Soc. London, Ser. A **381**, 17 (1982).
[24] M. Kardar, G. Parisi, and Y.-C. Zhang, Phys. Rev. Lett. **56**, 889 (1986).
[25] W. W. Mullins, J. Appl. Phys. **28**, 333 (1957); C. Herring, in *The Physics of Powder Metallurgy*, edited by W. E. Kingston (McGraw-Hill, New York, 1951).

[26] J. Villain, J. Phys. I **1**, 19 (1991).
[27] Z.-W. Lai and S. Das Sarma, Phys. Rev. Lett. **66**, 2348 (1991).
[28] F. A. Silveira and F. D. A. Aarão Reis, Phys. Rev. E **75**, 061608 (2007).
[29] T. J. Oliveira and F. D. A. Aarão Reis, Phys. Rev. E **76**, 061601 (2007).
[30] J. M. Kim and J. M. Kosterlitz, Phys. Rev. Lett. **62**, 2289 (1989).
[31] V. G. Miranda and F. D. A. Aarão Reis, Phys. Rev. E **77**, 031134 (2008).
[32] Y. Kim, D. K. Park, and J. M. Kim, J. Phys. A **27**, L533 (1994).
[33] F. D. A. Aarao Reis, Phys. Rev. E **70**, 031607 (2004).
[34] H. K. Janssen, Phys. Rev. Lett. **78**, 1082 (1997).
[35] M. E. R. Dotto and S. S. Camargo Jr., J. Appl. Phys. **107**, 014911 (2010).
[36] B. R. Conrad, W. G. Cullen, B. C. Riddick, and E. D. Williams, Surf. Sci. **603**, L27 (2009).
[37] J. Kim, N. Lim, C. R. Park, and S. Yim, Surf. Sci. **604**, 1143 (2010).
[38] G. Zhang, B. L. Weeks, and M. Holtz, Surf. Sci. **605**, 463 (2011).